Inductively coupled plasma application in CW Laser Propulsion

Takayoshi Inoue[*], *Kohei Kojima*[*], *Susumu Uehara*[*], *Kimiya Komurasaki*[†], *Yoshihiro Arakawa*[*]

[*]*Department of Aeronautics and Astronautics, University of Tokyo*
7-3-1, Hongo, Bunkyo-ku, Tokyo 113-8656, Japan

[†] *Department of Advanced Energy, University of Tokyo*
7-3-1, Hongo, Bunkyo-ku, Tokyo 113-8656, Japan

t.inoue@al.t.u-tokyo.ac.jp

Keywords: Laser Propulsion, Inductively Coupled Plasma, RF, Plasma Interaction

Abstract

A concept in which laser-sustained plasmas (LSPs) are combined with inductively coupled plasmas (ICPs) is proposed. The concept is aiming at extensions of operative conditions of a CW laser thruster due to the fact that the ICP has some characteristics which are in contrast to those of LSPs. An estimation confirmed that the concept would effectively work. And a fundamental experiment was conducted. The results showed that the radio frequency magnetic field induced by a alternate current of 13.56 MHz coupled inductively with LSPs, resulting in the enlargement of the plasma region and the attainment of the enthalpy. It is expected that some improvements will enable to transfer the RF power to the work gas more effectively and to demonstrate the synergy effect between the LSPs and the ICPs.

Introduction

Nowadays non-chemical propulsion has started to be used as the main propulsion system in space mission[1]. Laser propulsion has been investigated to develop a prospective propulsion system that may be used in space and in the atmosphere. Two kinds of laser propulsion have been proposed: CW (Continuous wave) laser propulsion[2] and RP(Repetitive-Pulsed) laser propulsion[3]. In these systems, a high power laser signal may be beamed to the spacecraft from remote sites, inducing the attainment of high propellant enthalpy.

Some of the most significant characteristics of the laser propulsion are the facts that power sources need not to be loaded onto the vehicle and that atmospheric air can be utilized as propellant especially for a launcher. Hence, its payload fraction is expected to become higher than that in other propulsion systems. In this study development of the CW laser propulsion is targeted.

The acceleration mechanism of the CW laser propulsion is as follows; the LSP absorbs the high power laser beam from a remote site, and is sustained in the propellant flow. The propellant gas is heated by the LSP, and the gas enthalpy is converted to thrust by a supersonic nozzle.

It is thought that Laser Orbital Transfer Vehicle (LOTV) is more feasible than the launcher from the aspect of the laser device development. The most important parameter for LOTV application is specific impulse. Any kind of element can be chosen as the propellant of the laser propulsion; especially by using the gas of low mass number such as hydrogen and helium, high specific impulse of the order of 1000 s will be achieved.

In the previous study, it was found that the smaller the mass flow rate of the propellant, the larger the specific impulse is. However it was shown that the decrease of the mass flow rate resulted in reduction of the efficiency due to decrease of the pressure. The lower limit of the pressure was about 1 atm. Aiming at the high specific impulse, the mixture of the argon and the helium was used as the work gas. The experiment showed that the LSP became unstable with the increase of the fraction of the helium, and the maximum mixture fraction was about 50 % in mole fraction.

In this study a new application of inductively coupled plasmas (ICPs) to the CW laser propulsion have been proposed, aiming at 1) an improvement of the stability of the CW laser thruster under an atmospheric pressure, and 2) a demonstration of the operation using the helium as the propellant. A fundamental experiment was conducted.

LSPs supported by ICPs

Inductively coupled plasma

Application of radio-frequency (rf) inductively coupled plasma technique has increased enormously since the development of the today's ICP torches by Reed[5,6]. This type of plasma is used in many disciplines for destruction of waste material, as a plasma source of atomic excitation in analytical chemistry, materials processing, spray coating of metals and ceramics, chemical vapor deposition of diamond films, and nucleation and growth of sub-micron powders. Even in the field of the astronautics, an induction coupled plasma torch had been researched to simulate various aspects of the Gas Core Nuclear Rocket[7-9].

ICPs have some characteristics which are in contrast to those of LSPs.

- ✓ easiness of discharge in the helium gas
- ✓ stable over a wide range of a pressure, especially under an atmospheric pressure.

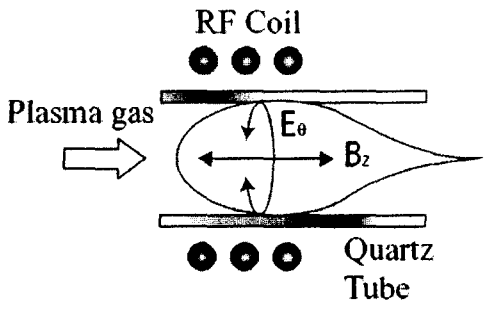

Fig. 1. Mechanism of the inductively coupled plasma.

ICP is generated in a radio frequency (RF) alternate magnetic field as shown in fig. 1. The ICPs differ from the LSPs in discharge properties; the minimum sustaining power of the ICPs decreases with the decrease of the pressure. Hence the ICPs have potentials to extend the operative conditions of the CW laser thrusters.

In addition to the feature at low pressure, helium inductively coupled plasmas, operated at atmospheric pressure, have been generated by the RF power of 400 W[12] while the generation of helium LSP have not achieved yet in our previous investigation.

Concept of the application of ICP

The LSP involves a propagation phenomenon of a high temperature region, where the laser beam is absorbed, in a flowing filed[10]. The decrease of the absorption coefficient with the decrease of the pressure or the increase of the fraction of the helium leads to the lack of the energy to maintain the LSP, and resulted in the LSP vanishing. Hence, it is expected that addition of a mechanism which increases the absorption coefficient extends the operational conditions.

Most of the laser propulsion researches have employed the CO_2 laser devices because of the capability to provide high power beam. The wavelength of 10.6 μm of the CO_2 laser is too large to ionize atoms by the multi-photon process, and the inverse bremsstrahlung process must be dominant for the absorption process of the CO_2 laser.

The absorption coefficient of the process is proportional to the electron number density[11]. Therefore, in order to increase the absorption coefficient, increase of the electron number density will be effective. An ICP will be good source to provide the additional electrons to support the laser absorption. A schematic diagram of the concept is shown in fig. 2.

This concept involves two potential features;

1. To sustain the LSP under the pressure of 1atm.
2. To use helium as propellant

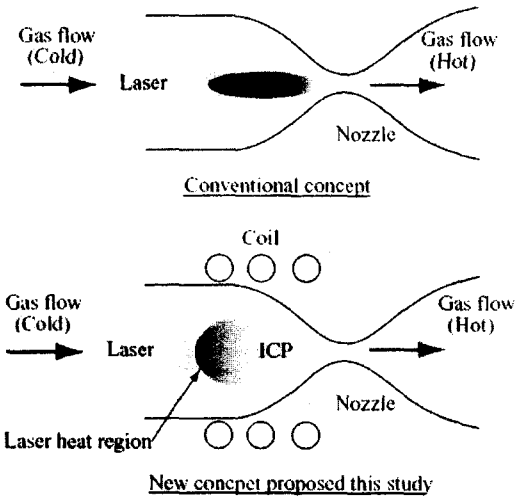

Fig. 2. Schematic diagrams of the laser absorption processes; conventional cw laser thrusters (upper) and the proposed concept (lower).

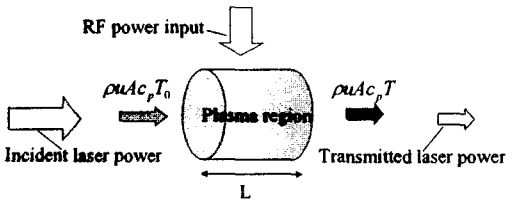

Fig. 3. Schematic of the model for the estimation.

1-D estimation of laser absorption

In order to validate the concept, the rate of the laser absorption was estimated. Figure 3 shows a schematic diagram of a model for the estimation. Assuming that the temperature of the plasma is uniform over the plasma region and that the RF power, which generates the ICP, is transmitted to the work gas without losses, the equation of the energy balance can be expressed;

$$\rho u A C_p T + q_{rad}(T) A L = P_{ICP} + P_{Laser}\left[1 - \exp\left(-k(T)L\right)\right] \quad (1)$$

where ρ: density, u: velocity of the flowing fluid, A: cross section, C_p: specific heat at constant pressure, L: length of the plasma region, q_{rad}: radiation power per unit mass, P_{ICP}: RF power input, P_{Laser}: laser power, k: absorption coefficient. We took into account the inverse bremmstrahlung radiation and the black body radiation for the absorption process and the radiation process respectively. It was assumed that the length of the plasma region was 50 mm, and the work gas was Argon.

The results of the estimation are shown in fig. 4 and 5, where the pressures were 0.1 MPa and 0.05 MPa respectively. The effect of the RF power appears more significantly in the 0.05 MPa case than in the 0.1 MPa case.

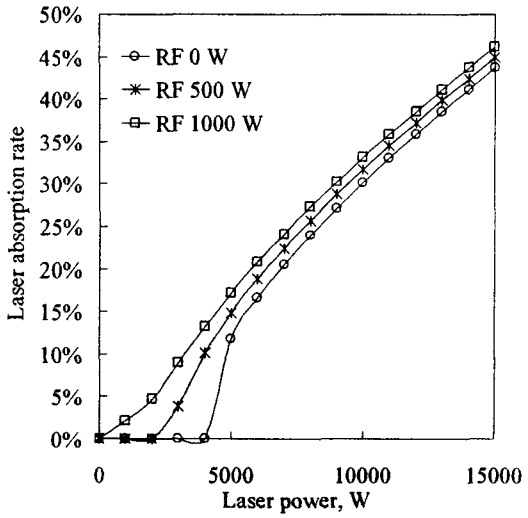

Fig. 4. Estimated laser absorption rate vs. the laser power; the pressure was 0.1 MPa.

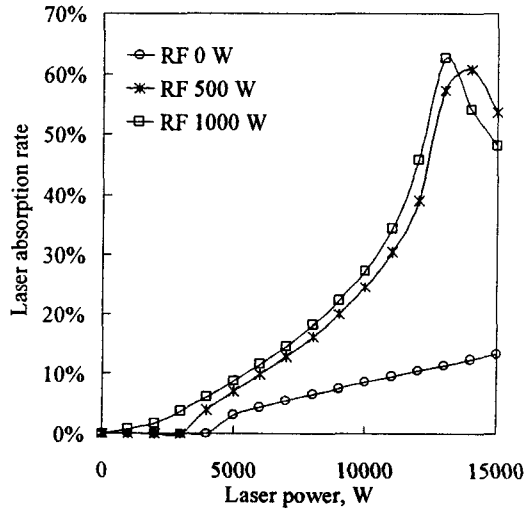

Fig. 5. Estimated laser absorption rate vs. the laser power; the pressure was 0.05 MPa

Experimental Setup

ICP torch

Figure 6 shows a schematic of the experimental apparatus. The apparatus was composed of a laser induction window, a plasma-sustaining channel and a laser exit window. A zinc selenide (ZnSe) disk with anti-reflection coating was used as the windows. The aperture diameter of the window was 35 mm and the thickness was 7 mm. The ZnSe window has high transmission efficiency over the far infrared region involving around 10.6 μm wavelength. A quartz glass tube as the plasma-sustaining channel was supported by a set of holders made of stainless steel, enabling generation of the ICP and observation of the plasma . The inner diameter of the tube was 22 mm. Argon was used as the work fluid in this study.

The work gas was pumped out through an orifice by an oil-sealed rotary vacuum pump in order to regulate the pressure in a wide rage, although most of the atmospheric ICP torch have been generated in an open tube. The pumping speed of the pump is 80 m^3/h and the diameter of the orifice was 1.3 mm. The pressure of the plasma generation section is determined by flow choking in the orifice.

The objective of this study is to investigate the effects of the RF field on the LSP. Hence the LSP should be generated before the RF field is applied. A rod made of stainless steel was used as the source of the initial electron emission. After the ignition the LSP was moved into the plasma-sustaining channel with a movement of the focal point. The rod mounted on an air cylinder can be taken in and out

The static pressure in the tube was measured with a semiconductor pressure transducer (Philips Sensor Technology Corp.: JS-24SHD-10). The holder of the quartz tube is water-cooled

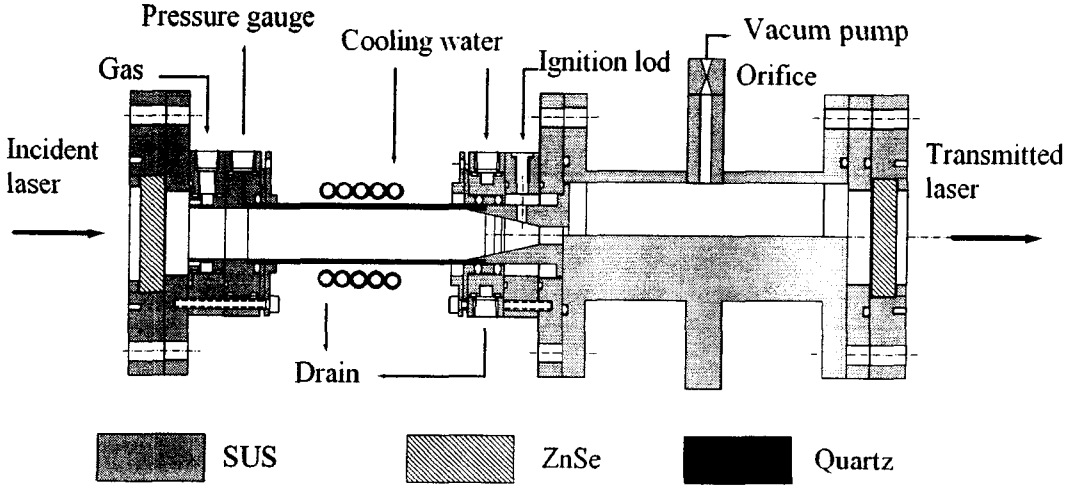

Fig. 6. Cross section of the ICP torch.

Power supply and IMN

A 1.25kW RF power supply (ENI Technology Inc. OEM-12) was employed to generate RF field. The frequency of the RF power supply is 13.56 MHz and the maximum reflected power is 300 W. A water-cooled load coil, fabricated from 3 mm copper tubing, has an inside diameter of 30 mm and consists of 5 turns. The coating of the copper tubing with a thermal shrinkage tube eliminates the problem of the short-circuiting between respective turns.

A matching circuit (Thamway Co.,Ltd. T020-6066C) was used, which is a manual system. The circuit diagram is shown in fig. 7. The matching circuit is composed of the load coil, a capacitor, and two variable capacitors; one of the variable capacitors is connected to the coil in series and the other in parallel.

The forward power and the reflected power are read out from the RF power supply. The dissipated RF power is obtained by subtracting the reflected power from the forward power

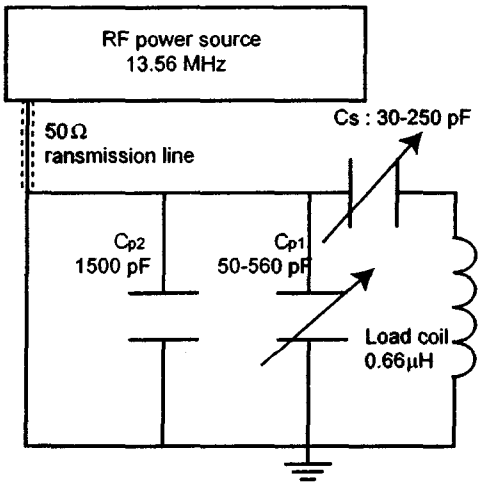

Fig. 7: Impedance matching network for a 13.56 MHz RF power supply.

CW CO_2 laser

A 2kW CW-CO_2 laser (Panasonic YB-L200B7T4) was utilized. The transverse mode of the laser beam is TEM10*. The beam divergence is less than 2 mrad at the laser exit. The beam diameter was magnified by factor of 2.2 using a ZnSe beam expander, and the expanded beam was condensed into the discharge tube through a ZnSe plano-convex lens. The focal length of the lens was 210 mm, corresponding to 6.3 in F-number (which was defined as focal length normalized by beam diameter). The effective laser power which incident to the test section was 560 W for the laser power of 700 W due to the attenuation by the optics system.

Setup and experimental procedure

Figure 8 shows a schematic diagram of the experimental apparatus. In these experiments, The ICP torch was placed on a precision jack and has two pin holes in front and behind, which can be removed during experimentations, in order to adjust the axis of the torch to that of the laser beam. The working gas was argon and its flow rate was 0.45 g/s.

Assuming that the static pressure is equal to the stagnation pressure due to the fact that the flowfield velocity of the measuring point is enough small, the stagnation temperature T_0 was calculated using eq. (2) where A_e is the cross section of the orifice, P_0 is the stagnation pressure, $\dot{m}$ is the mass flow rate and σ (=0.726 for monatomic gas) is the critical flow coefficient. The thermal efficiency of the RF power was defined as eq. (3), where the T_{LSP} is the stagnation temperature when the RF power was 0 W, C_p is the specific heat at constant pressure, and the P_d is the RF dissipated power.

$$T_0 = \frac{1}{R}\left(\frac{A_e P_0 \sigma}{\dot{m}}\right)^2 \tag{2}$$

$$\eta_{RF} = \frac{\dot{m} c_p (T_0 - T_{LSP})}{P_d} \tag{3}$$

The propellant flow rate was regulated with a mass flow controller. The transmitted laser energy through the exit window was monitored using a calorimeter (Coherent: LM-5000). The signals from these sensors were recorded with an eight channel digital oscilloscope (Yokogawa Electric Corp.: DL-708).

The measurements were carried out three times for each parameter and the mean values and the standard deviations of the measured values were calculated.

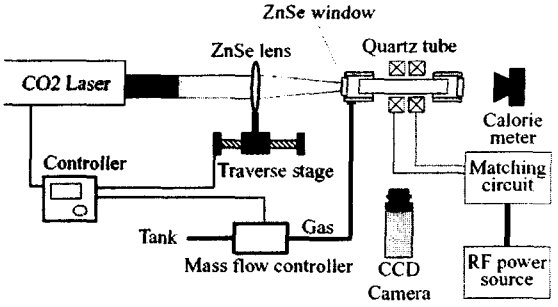

Fig. 8. Experimental setup.

Results and Discussion

In order to work out the effect of the RF field on the LSP, the RF field was applied to the LSP, which had been produced inside of the load coil.

Experimental procedure was as follows:

a) Injection of the work gas.
b) LSP ignition and move the LSP to be inside of the load coil.
c) RF power-on.
d) Laser and RF power-off.

Before the LSP ignition the flow rate was set up at 0.51 g/s to initiate the LSP stably. As the LSP had

been initiated, the flow rate was regulated up to experimental conditions. Figure 9 shows typical signals of the pressure and the RF reflected power. The laser power was 700 W and the RF forward power was 880 W. The graph shows that increment of the RF forward power resulted in the increasing of the pressure and also the laser transmittance (c-d). The observation of a CCD camera is shown in fig. 10. After the ignition of the LSP it was located inside of the load coil (B in fig. 10). Then the RF field was applied (C in fig. 11). It was found that the LSP was heated by the RF magnetic field and the luminous region expanded by a factor of 5. As the luminous intensity of the expanded region was smaller than that of the LSP, it is thought that the temperature of the region is lower than that of the LSP. These features can be considered to be just the characteristics of the ICP.

The stagnation temperature calculated from eq. (2) is shown in fig. 11, the RF forward power of 0 W corresponding to the operation just of the LSP. The result shows that the stagnation temperature increases linearly with the increase of the RF dissipated power. As shown in fig. 12, the thermal efficiency of the RF heating was about 6 % while that of the LSP was about 3 %. The optimization of the diameters of the coil and discharge tube will improve the efficiency[13].

Figure 13 shows the RF reflected power. The result shows that there is admit of improvement to ensure the efficient transfer of the RF power. The capacitances of the C_p and C_s that minimizes the reflected power are tabulated in table 1. The mismatching between the power source and the IMN seemed to be resulted from the limit of the variable range of the capacitor C_p.

The experiments observed that the laser absorption decreased slightly rather than that the laser absorption increased. However it is expected that the improvements of the IMN and the coil configuration will enable to transfer the RF power to the work gas more effectively and resulted in the synergy effect between the LSPs and theICPs.

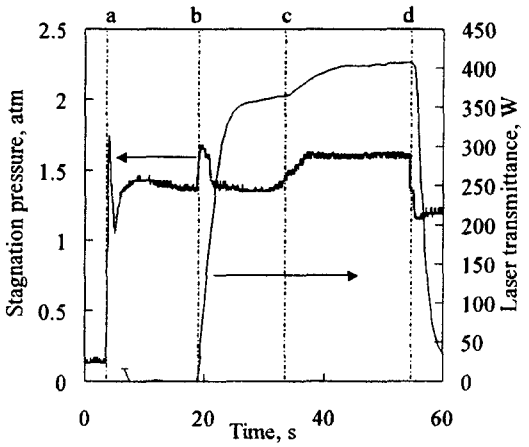

Fig. 9. Typical signals of the pressure and the laser transmittance.

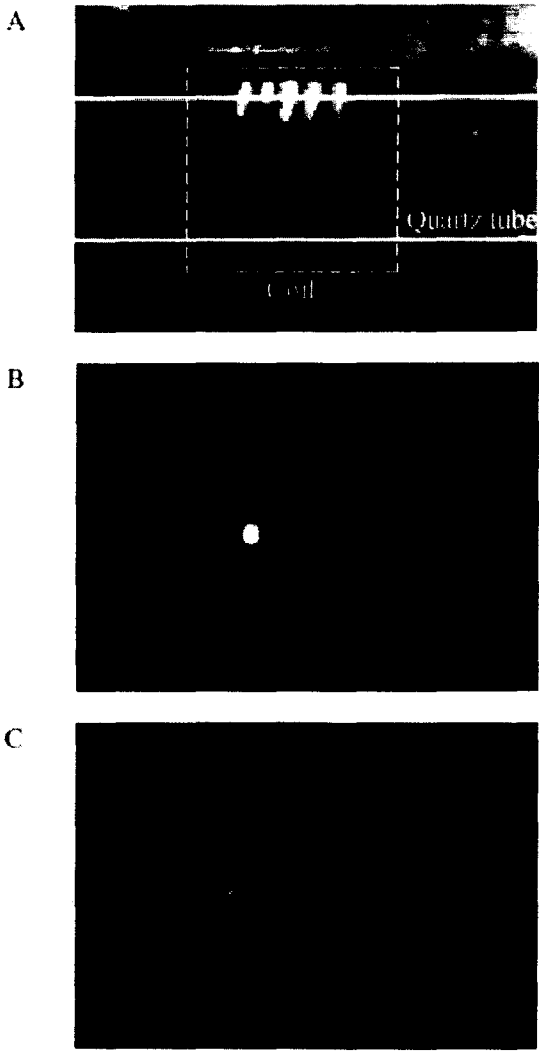

Fig. 10. Observation of the CCD camera: A) Overview of the discharge tube and its holder, B)Laser-sustained plasma without RF effect (laser power: 700W), C)Laser-sustained plasma applied the RF power of about 700 W.

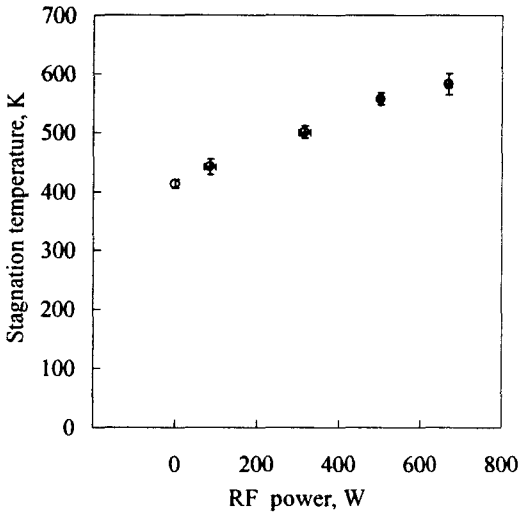

Fig. 11. Stagnation temperature vs. RF forward power.

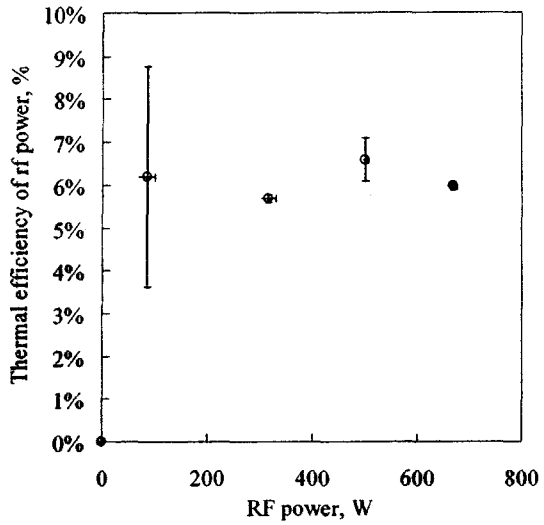

Fig. 12: Thermal efficiency of RF power.

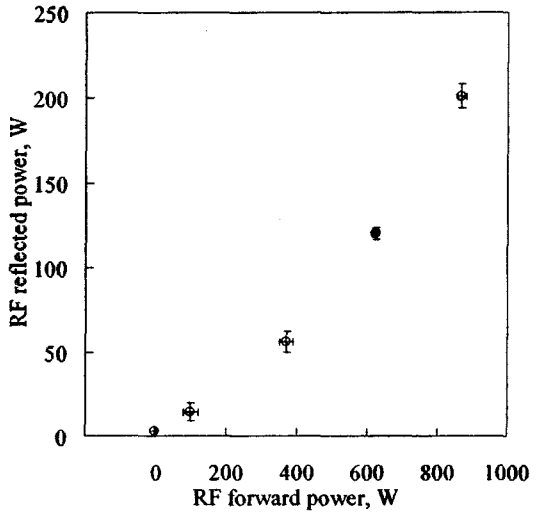

Fig. 13. RF reflected power vs. RF forward power.

Table 1. The values of the capacitors; C_p is the sum of the C_{p1} and C_{p2}. "Without the LSP" corresponds to the case of the LSP being not in nor in the vicinity of the load coil. "With the LSP" to the case of the LSP being inside the coil.

	C_s	C_p
without the LSP	147	1995
with the LSP	149	1500

Conclusion

- A concept aiming at extensions of operative conditions of a CW laser thruster was proposed.
- An estimation confirmed that the concept would effectively work.
- A fundamental experiment was conducted.
- The LSP was heated by the RF field and the volume of the plasma region expand significantly

References

1) J.Kawaguchi: The Muses-c Mission for ther Sample and Return – Its Technology Development Status and Readiness, *Acta Astronoat.*, **52**, 2003, pp.117-123.
2) K.Toyoda, etal..: Thrust Performance of a CW Laser Thurster in Vacuum, *Vacuum*, **65**, 2002, pp.383-388.
3) T.S.Wang et.al.: Advanced Performance Modeling of Experimental Laser Lightcraft, J. Propulsion Power, **18**, 2002, pp.1129-1138.
4) A.Sasoh: Laser-driven in-tube accelerator, Rev. Sci. Instrum., 72, 2001, pp.1893-1898.
5) T.B.Reed: Induction-Coupled Plasma Torch, *J. Appl. Pys.*, **32**, 1961, pp.821-824.
6) T.B.Reed: Growth of Refractory Crystals Using the Induction Plasma Torch, *J. Appl. Phys.*, **32**, 1961, pp.2534-2535.
7) M.L.Thope, et.al.: Induction Plasma Heating, *NASA-CR* 1343, 1969.
8) E.Charles, et.al.: Radiation Measurements and Low Frequency and High pressure Investigations of Induction Heated Plasma, *NASA-CR* 1807, 1971.
9) W.John, et.al.: Induction Torches and Low Frequency Tests, *NASA-CR* 2053, 1972.
10) Raizer, Y.P.: Laser-Induced Discharge Phenomena, Plenum pub. Corp., New York, 1977, pp. 180-188.
11) N.H.Kemp, et.al.: Laser-Heate Thruster – Interim Report, *NASA-CR*, 161665, 1980.
12) T.Okino, et.al.: Enhanced vortex flow torch for a helium ICP, *BUNSEKI KAGAKU*, 43, 1994, pp.377-382. (*in Japanese*).
13) H.U.Eckert: Analysis of thermal induction plasmas dominated by radial conduction losses, J.Appl.Phys, **41**, 1970, pp.1520-1528.